ARTICLES

State-Resolved Photofragmentation of $[ClNO]_n$ van der Waals Clusters in a Supersonic Jet

Carlos Conde,[†] Christof Maul,[‡,§] and Edwin Quiñones*

Department of Chemistry, University of Puerto Rico, P.O. Box 23346, San Juan, Puerto Rico 00931-3346

Received: October 8, 1998; In Final Form: February 3, 1999

The effects of the ultraviolet laser irradiation of $[ClNO]_n$ weakly bound clusters, formed in a supersonic jet, are analyzed by considering three processes: the photofragmentation of bare ClNO, the Cl + ClNO reaction, and NO relaxation within the cluster. The photofragmentation of jet-cooled ClNO at 355 nm produces NO($v'' = 1$) with a kinetic energy of 2240 cm^{-1}, a spin−orbit preference of $F_1/F_2 = 1.2$, and Λ-doublet state preferences of $\Pi(A'')/\Pi(A'') = 2.0$ and 4.0 for the F_1 and F_2 manifolds, respectively. The NO distribution of rotational states was parametrized using a Gaussian function centered at $N = 34$, with a fwhm of 17. On the other hand, the Cl + ClNO reaction, studied at a collision energy of 2780 cm^{-1}, gives NO($v'' = 1$) described by a Boltzmann rotational distribution with $T_{rot} = 950 \pm 100$ K. The relative population of the NO spin−orbit states is $F_1/F_2 = 2.5$, with a Λ-doublet state preference of $\Pi(A'')/\Pi(A') = 1.2$ and E_{trans}(NO) of 578 cm^{-1}. It is found that 57% of available energy is disposed as $E_{int}(Cl_2)$. As a result of the irradiation of the $[ClNO]_n$ clusters at 355 nm are observed: Boltzmann ensembles of NO($v'' = 1$) and NO($v'' = 0$) molecules described by T_{rot} of 310 ± 30 and 170 ± 25 K, respectively, with no spin−orbit or Λ-doublet state preferences, overlapped with a Gaussian distribution already assigned to the NO photofragment. The relative contribution of the NO($v'' = 1$) photofragment to the spectra is drastically reduced upon increasing the backing pressure, as it undergoes translational and rotational relaxation within the clusters. Our high-resolution studies provide evidence that suggests that the reaction takes place within the $[ClNO]_n$ clusters.

I. Introduction

Beyond their intrinsic importance, van der Waals complexes provide us with the prospect of studying chemical processes in environments with unprecedented physical properties.[1,2] While in the past it was necessary to disregard those factors that do not have a direct influence on the outcome of elementary reactions, these weakly bound clusters are now amenable to explicitly consider the individual interactions between the reactants and the surrounding solvent molecules during the trajectory of a collision.[3,4] The understanding that has emerged of the solvation problem together with the tremendous progress achieved in the past two decades on the characterization of molecular interactions employing spectroscopic and theoretical methods, has encouraged this research direction.[5−7]

Through the appropriate choice of the gas expansion conditions it is possible to favor the formation of binary van der Waals (vdW) precursors to study photochemical reactions. Solvent effects do not play a role in this class of experiments, and the results derived from them aim at improving the understanding of the dynamics of elementary molecular collisions. In particular, in the investigation carried out by Wittig and co-workers on the H + CO_2 reaction preparing the BrH−CO_2 vdW precursor, they found that OH is produced rotationally colder than when the same reaction was studied under bulk conditions because the range of impact parameters available to the reaction is narrowed as a consequence of the stereochemical control of the collision.[8] On the other hand, Sauder et al. in their study of the $^{16}O(^1D) + H_2{}^{18}O$ reaction, photoinitiated within the O_3−H_2O vdW complex, determined the rotational distributions of the two OH products, one of which carries the information of the newly formed bond.[9] They concluded that a significant fraction of the available energy to the reaction is removed by O_2, the other product of the photolysis of ozone, before departing from the collision region. Studies of reactions involving vdW molecules containing metal atoms initiated with polarized laser light have contributed enormously to the understanding of orbital alignment effects in chemical reactions as exemplified by the work of Breckenridge, Soep, Jouvet, and co-workers.[10,11] Moreover, vdW complexes have been the subject of energy transfer studies, which should be mentioned: the vibrational-to-translational energy transfer investigation within the HF−NO vdW complex carried out by Shorter et al.,[12] the study of Honma et al.[13] of the atom + diatomic inelastic collisions within the $[NO]_2$ vdW complex, and predissociation studies of van der Waals molecules.[14−17]

Reactions initiated in vdW clusters tend to display the behavior observed in the liquid state as the cluster size increases.[1] Garvey and Bernstein studied reactions of methyl halides induced by electron impact ionization in the environment of weakly bound clusters.[18] This was the first experimental

[†] Present address: SmithKline Beecham Pharmaceuticals Co., P.O. Box 11975, Cidra, Puerto Rico 00639-1975.

[‡] Present address: Institut Für Physikalische und Theoretische Chemie, Technische Universität Braunschweig, Hans-Sommer-Strasse 10, D-38106 Braunschweig, Germany.

[§] Fellow of the Deutsche Forschungsgemeinschaft.

* Address correspondence to this author.

10.1021/jp9840127 CCC: $18.00
Published on Web 03/12/1999

attempt to test whether the existing kinetic theories that describe the behavior of ion−molecule reactions could be employed to explain their behavior within clusters. Sivakumar et al. carried out a photofragmentation investigation of $[OCS]_n$ clusters. In their work, OCS was the light absorbing species, $OCS + h\nu \rightarrow S(^1D) + CO$, and carbon monoxide was detected rotationally and vibrationally cool as a consequence of the relaxation process in the clusters. Sivakumar et al. observed the $S(^1D) + OCS \rightarrow S_2 + CO$ reaction within the $[OCS]_n$ clusters by monitoring the S_2 molecule and concluded that this reaction was another source of CO.[19] Bergmann and Huber photodissociated methyl nitrite, $CH_3ONO + h\nu \rightarrow CH_3O + NO$, solvated in large $[CH_3ONO]_n$ clusters and detected NO from the photodissociation of bare CH_3ONO, NO rotationally relaxed emanating from the clusters, and the $CH_3O + NO \rightarrow HNO + H_2CO$ disproportionation reaction.[20] Jones et al. found that the elimination of SF_6 was the dominant process during the infrared photofragmentation of $SF_6[C_6H_6]_n^+$ clusters.[21] Ning and Pfab studied the photodissociation of nitrous acid embedded in water clusters and determined a bimodal NO rotational distribution corresponding to the cases when HONO was electronically excited under collisionless conditions and within the water clusters, respectively.[22] On the other hand, Rudich et al. found that cyclohexanol (the product observed in liquid cyclohexane) is formed when the $O(^3P) + C_6H_{10}$ reaction was carried out in cyclohexane clusters, while the OH and cyclohexyl radicals are the products formed under single collision conditions, clearly indicating that the abstraction mechanism is suppressed by the cluster cage.[23]

In this paper we present a study of the dynamics of the photofragmentation of $[ClNO]_n$ weakly bound clusters at 355 nm, formed in a supersonic jet. Working under expansion conditions at which the clusters are formed, we observed nitric oxide (1) that has undergone translational, rotational, and spin−orbit state relaxation, (2) that is from the ClNO photofragmentation, and (3) that is from the Cl + ClNO reaction. High-resolution measurements allowed us to assign the contribution of the three basic processes to different regions of the NO fine structure spectra. To understand the photofragmentation of the $[ClNO]_n$ clusters, we carried out studies under bulk conditions of the dynamics of the photofragmentation of ClNO and of the Cl + ClNO reaction.

II. Experimental Section

A. Description of the Apparatus. Our apparatus consists of a 12 in diameter stainless steel chamber coupled to a Varian VHS-10 diffusion pump, pumped by a 39 cfm mechanical pump. A pulsed solenoid valve (General Valve Series 9) with a 0.8 mm nozzle diameter was used to expand the ClNO/He mixtures and the reactions were observed at 25 nozzle diameters downstream. The pressure in the chamber was about 1×10^{-6} Torr before operating the pulsed valve and never was above 1×10^{-4} Torr when the valve was operated at 10 Hz at backing pressures up to 6 atm. A Nd:YAG laser (Continuum Surelite II) in its third harmonic (355 nm) was utilized to photodissociate ClNO using laser pulses of 3 mJ. The photolysis laser beam was focused onto an area of 1 mm^2 using a 100 cm focal length lens. The dye laser (Lambda Physik LPD 3002) was pumped by an excimer laser (Lambda Physik LPX 205i) operating at 308 nm. The dye was Coumarin 460 (Aldrich), and the beam was frequency doubled by a BBOI doubling crystal. The dye laser beam was collinearly counter propagated to the photolysis laser to probe the fine structure of NO. The NO molecules were detected by using probe laser pulses of less than 5 μJ in order to avoid optical saturation. A time delay of 50 ns between the photolysis and the probe laser was controlled by a digital delay and pulse generator (Stanford Research DG535). The laser-induced fluorescence (LIF) signal was viewed by a frontal PMT (Thorn EMI), coupled to a 300 MHz digital oscilloscope (LeCroy 9450A), integrated by a boxcar (Stanford Research SR 250), fed into a Macintosh IIci computer, and interfaced to a GW Instrument MacAdios II card, programmed with MPW FORTRAN. Each data point was averaged for at least 10 laser pulses, and the spectra were corrected for variations in the dye laser output energy as a function of wavelength. The dye laser resolution was adjusted to ensure that each rotational line was defined by at least five data points. Prior to every experimental run, the 0−0 band origin of the $A^2\Sigma^+ \leftarrow X^2\Pi_{1/2}$ transition in NO was monitored in order to establish low-temperature conditions. We detected the emission emanating from the photodissociation of the NO−Ar vdW complex around 224 nm to optimize the delay between the pulsed valve and the photolysis laser to ensure cluster formation conditions.[24]

An intracavity Etalon was installed to scan individual rotational lines. A resolution of 0.04 cm^{-1} in the UV region was confirmed by scanning the rotational lines of jet-cooled NO.

ClNO was prepared by mixing 3:1 samples of NO and Cl_2 (Air Products) in the presence of room light, allowing 20 min for the mixture to reach equilibrium. The excess NO was pumped out after cooling the sample using a dry ice/methanol slush. Typical samples consisted of 3% ClNO in He at total pressures ranging from 1 to 6 bar.

The experiments in the bulk were done in the molecular beam chamber by shutting off the gate valve and adding 150 mTorr of ClNO.

B. Spectroscopic Simulations. The experimental distributions of $NO(v'' = 0,1)$ rotational states were derived using computer simulations of the $NO[A^2\Sigma^+(v' = 0) \leftarrow X^2\Pi_\Omega(v'' = 1)]$ transitions. We showed for $v'' = 0$ that the integration of the lines and the simulations give the same results. We included 75 rotational states in our simulations. The following expression was employed to calculate the rotational energy of the $A^2\Sigma^+$ state,

$$\tilde{\nu}_A = N(N+1)\tilde{B}_0' - N^2(N+1)^2\tilde{D}_e' \quad (1)$$

where N stands for the rotational quantum number excluding the electron spin according to Hund's case (b), $\tilde{B}_o'$ is the rotational constant in $v' = 0$, and $\tilde{D}_e'$ is the centrifugal distortion constant.[25] The rotational energy of the $X^2\Pi_{1/2}$ spin state (F_1 manifold) is given by[25]

$$\tilde{\nu}(J'')_{F_1} = \left[\left(J'' + \frac{1}{2}\right)^2 - 1 - \frac{1}{2}\sqrt{4\left(J'' + \frac{1}{2}\right)^2 + Y(Y-4)}\right]\tilde{B}_1'' - J''^4\tilde{D}_e'' \quad (2)$$

where $J = N + {}^1/_2$, A_1 is the spin−orbit constant, $\tilde{B}_1''$ is the rotational constant in $v'' = 1$, $\tilde{D}_e''$ is the centrifugal distortion constant, and $Y = A_1/\tilde{B}_1''$. The equation employed to calculate the rotational energy in the $X^2\Pi_{3/2}$ spin-state (F_2 manifold) was

$$\tilde{\nu}(J'')_{F_2} = \left[\left(J'' + \frac{1}{2}\right)^2 - 1 + \frac{1}{2}\sqrt{4\left(J'' + \frac{1}{2}\right)^2 + Y(Y-4)}\right]\tilde{B}_1'' - (J'' + 1)^4\tilde{D}_e'' \quad (3)$$

where $J = N - {}^1/_2$. The rotational distribution of the $NO(X^2\Pi_\Omega,$

$v'' = 1$, J'') states emanating from the photofragmentation of ClNO at 355 nm was represented by a Gaussian type function

$$G(J'') = S_{J'',J'} \exp\left[-4 \ln 2\left(\frac{J'' - \tilde{J}''}{D(J'')}\right)^2\right] \qquad (4)$$

with a full width at half-maximum (fwhm) $\Delta(J'') = 17$ and a mean rotational state $J'' = 34.5$. The line strength factors for the $A^2\Sigma^+ - X^2\Pi_\Omega$ transitions are denoted by $S_{J'',J'}$ and we employed the formula available from the literature for Hund's intermediate case between (a) and (b) because we are detecting high NO rotational states.[26] On the other hand, the distributions of rotational states of NO emanating from the ClNO + Cl reaction as well as NO relaxed due to its interaction with the clusters were parametrized using a Boltzmann function. The line shapes were represented using a Gaussian function with a constant fwhm of 0.4 cm^{-1}. The computer code was tested using a laser excitation spectrum of thermal NO at 100 mTorr. No aligment effects were included in our analysis. We believe this should not change our qualitative interpretations.

III. Results and Discussion

A. Description of the Photofragmentation of ClNO at 355 nm. The conclusions that one can reach about the dynamics of the photofragmentation of $[ClNO]_n$ clusters, involving ClNO as the light absorbing species, strongly depend on the previous knowledge of the dynamics of the photofragmentation of bare ClNO at 355 nm. In accordance, we summarize here the most relevant findings about ClNO photofragmentation.

Nitrosyl chloride presents an absorption spectrum in the 200−600 nm range consisting of several dissociative singlet and triplet states.[27,28] The photodissociation cross-section of ClNO (D_0 = 13 030 cm^{-1}) at 355 nm (E = 28 169 cm^{-1}) is, $\sigma = 1.36 \times 10^{-19}$ cm^2, and the quantum yield for the formation of NO and Cl equals unity.[29,30] Bai et al. found that in the photodissociation of ClNO, $ClNO + h\nu \rightarrow NO(^2\Pi_\Omega, v'', J'') + Cl(^2P_j)$, the spin−orbit states in which Ω equals j are preferentially produced, as confirmed by Chichinin detecting the individual j states of chlorine and by Huber and co-workers detecting the NO molecule.[27,31−33] In particular, the photolysis of ClNO at 355 nm has the propensity to produce the $Cl(^2P_{1/2})$ spin−orbit state, which is above $Cl(^2P_{3/2})$ by 881 cm^{-1}, and the $NO(^2\Pi_{1/2})$ spin−orbit states (i.e., $j = \Omega = {}^1/_2$). The $NO(^2\Pi_{3/2})$ manifold is 123 cm^{-1} above the $^2\Pi_{1/2}$ manifold. A recent examination of the UV photochemistry of ClNO monitoring the fine-structure branching ratio of the $Cl(^2P_j)$ atoms suggests the breakdown of this rule, due to nonadiabatic effects, when probing some regions of the ClNO potential energy surfaces.[34] Reisler, Huber, and co-workers observed NO Gaussian rotational distributions in their ClNO photodissociation studies at 355 nm.[27,32] At 355 nm the energy to be partitioned between the total center-of-mass translational energy of the photofragments and their internal energy is 15 139 cm^{-1}.[35] On the other hand, Reisler and co-workers assigned the ClNO absorption around 620 nm to a singlet−triplet transition. They observed that the ClNO parent molecule NO stretch evolves into NO vibrational excitation.[36]

The excitation of jet-cooled ClNO with linearly polarized laser light at 355 nm produces a spatial distribution of NO and Cl fragments described by an anisotropy parameter β of 1.8, consistent with a direct photofragmentation mechanism.[27] Busch and Wilson first determined that the electric dipole transition moment μ of ClNO is oriented parallel to the Cl−N bond in this band system and that 70% of the available energy is released into the translational degrees of freedom of the Cl and NO photofragments.[35] Accordingly, the NO rotational lines are broad.[27] The analysis of the photofragmentation dynamics of ClNO is simplified by rotationally cooling the parent molecule ($\mathbf{J}_{ClNO} \approx 0$) because the orbital angular momentum of the electronically excited Cl−NO collision complex, $\mathbf{L}_{Cl-NO}$, is approximately equal in magnitude (neglecting the photon and the Cl atom angular momenta) but has opposite orientation with respect to the rotational angular momentum of the NO fragment $\mathbf{J}_{NO}$ (i.e., $\mathbf{L}_{Cl-NO} \approx -\mathbf{J}_{NO}$).[37] The expression $P \propto \langle|\mu\cdot\epsilon|^2\rangle$ dictates that the NO photofragment is most likely ejected along the direction of the laser polarization vector ϵ in the laboratory frame because v_{NO} is parallel to μ. If one takes the direction of propagation of the probe laser $\mathbf{k}_{pr}$ as the quantization axis of $\mathbf{J}$ (the space-fixed Z axis) the NO molecules traveling along $\mathbf{k}_{pr}$ in a $\mathbf{J}$ angular momentum state can only exist in the $M_{pr} = 0$ substate, although the $2J + 1$ substates are populated for any other recoil directions.[38]

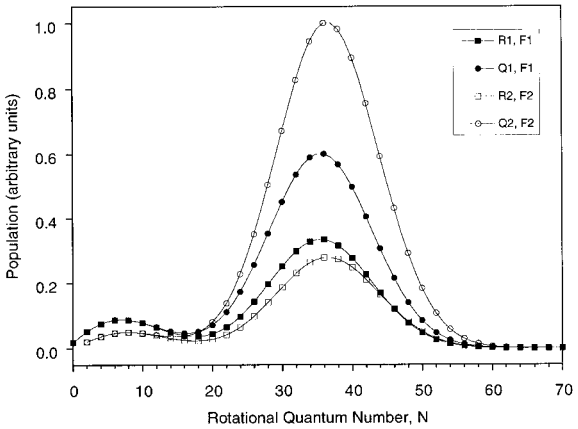

Figure 1. Distribution of rotational states of $NO(^2\Pi_\Omega, v'' = 1)$. The ratio of the spin−orbit state was $F_2/F_1 = 1.2$, and the Λ-doublet state relative populations $\Pi(A'')/\Pi(A')$ were 2.0 and 4.0 for the F_1 and F_2 manifolds, respectively.

B. Photofragmentation of ClNO at 355 nm under Bulk Conditions. We carried out a study of the photofragmentation of ClNO at 355 nm under bulk conditions to understand the role played by the photolysis of the ClNO monomer in our experiments. We centered our analysis mainly on $v'' = 1$ instead of $v'' = 0$ to minimize the detection of thermal NO, yet there is more overlap among the rotational branches in $v'' = 1$. In fact, a detailed study of the $v'' = 0$ level at the same wavelength has been reported by Reisler and co-workers.[27] We derived the relative populations of the Q_1, R_1, Q_2, and R_2 branches from the laser excitation spectrum of $NO(v'' = 1)$ produced from the excitation of 150 mTorr of ClNO at 355 nm, and the result is displayed in Figure 1. The spin−orbit state population ratio was $F_1/F_2 = 1.2$, while the ratio of the Λ-doublet state populations $\Pi(A'')/\Pi(A')$ were 2.0 and 4.0 for the F_1 and F_2 manifolds, respectively. The distribution of rotational states was parametrized using a Gaussian function, as defined in the Experimental Section, with the spin−orbit and Λ-doublet state preferences specified above. The Gaussian component extends from N equals 16 to 60, peaking at $N = 34$, with a fwhm equal to 17. We observed a small contribution of thermal NO in $v'' = 1$ below $N = 16$, centered around $N = 8$, although it does not appreciably overlap with the Gaussian component and does not affect our analysis of the photofragmentation process. A 300 K Boltzmann distribution was used to account for the small amount of thermal NO present, which we confirmed by scanning the dye laser while blocking the photolysis beam. Bai et al. determined a Gaussian rotational distribution with a mean N

value of 46 in their analysis of NO($v'' = 0$) from the photolysis of ClNO at the same wavelength.[27]

In the $^2\Sigma^+ - {}^2\Pi$ band system, the main-branch Q lines probe levels of $\Pi(A'')$ symmetry, while main-branch P and R lines probe $\Pi(A')$ states.[39,40] As Figure 1 shows, the photodissociation process produces preferentially the $\Pi(A'')$ (antisymmetric) Λ-doublet states in both manifold and this is because the fragmentation process is confined to a plane containing the three atoms.[39] The larger Λ-doublet state preference in the F_2 manifold explains why this manifold appears more populated. This experiment also establishes that there is no significant relaxation of the NO photofragment working at a ClNO pressure of 150 mTorr detecting NO with a delay time of 50 ns.

The Λ-doublet and spin-state preferences observed from the photodissociation of ClNO are fingerprints that will allow us recognize the presence of the NO photofragment under expansion conditions at which clusters are formed and to identify relaxation processes.

C. Dynamics of the Cl + ClNO Reaction under Bulk Conditions. Chlorine atoms are produced during the laser irradiation of the $[ClNO]_n$ clusters, and an aim of the present work is to determine whether the Cl + ClNO reaction takes place within these clusters. To this end, we studied this reaction under bulk conditions, since little is known about its dynamics.[41−45]

Grimley and Houston observed the participation of the Cl + ClNO reaction in their photolysis studies of ClNO in the 480−520 nm wavelength region, detecting infrared (IR) chemiluminescence from NO($v'' = 1$).[43] These workers found evidence that supports the following mechanism,

$$ClNO + h\nu \text{ (visible light)} \rightarrow Cl + NO \quad (5)$$

$$Cl + ClNO \rightarrow Cl_2 + NO \quad (6)$$

When the photolysis was carried out with visible light, they noted that reaction 5 did not contribute to the IR emission, as NO is mainly formed in $v'' = 0$, and measured the rate constant for the secondary process to be $(5.40 \pm 0.47) \times 10^{-12}$ cm^3 molecules^{-1} s^{-1}, monitoring NO($v'' = 1$). In contrast, they observed NO($v'' = 1$) instantaneously from reaction 5 when ClNO was irradiated at 355 nm. The Cl + ClNO reaction was used by Clyne et al. to measure the Cl atom concentration in discharge flow systems.[44]

We investigated the Cl + ClNO reaction under bulk conditions using a 2:1 mixture of Cl_2 and ClNO to favor the photolysis of Cl_2 as the Cl atom source. Although the magnitude of the absorption cross sections at 355 nm of Cl_2 and ClNO are similar, we used an excess of Cl_2 to favor reaction 6, which combines with the fact that the Cl_2 photodissociation produces two Cl($^2P_{3/2}$) atoms. On the other hand, the ClNO photodissociation at 355 nm contributes Cl($^2P_{1/2}$) atoms, but with a much broader distribution of translational energies.

A laser excitation spectrum of NO($v'' = 1$) from the photolysis of the Cl_2/ClNO mixture at a total pressure of 150 mTorr is presented in Figure 2A. A Boltzmann rotational distribution with a "temperature" of 950 ± 100 K describes this ensemble of NO molecules, which was determined from the simulation presented in Figure 2B. The "rotational temperature" allows the calculation of the average energy disposed by the reaction into NO($v'' = 1$) rotational energy, $E_{rot}(NO) \approx 660$ cm^{-1}. The reaction also presents a small Λ-doublet state preference of $\Pi(A'')/\Pi(A') = 1.2$. The relative population of the spin−orbit states is $F_1/F_2 = 2.5$, as can be noted from Figure 3. A Gaussian component was also used in the simulation to account for the small amount of ClNO photolyzed. The spin-state and Λ-doublet state preferences incorporated to the NO($v'' = 1$) Gaussian component were the same ones previously specified for the NO photofragment. The populations of the main branch R and Q transitions derived from the simulation are plotted in Figure 3.

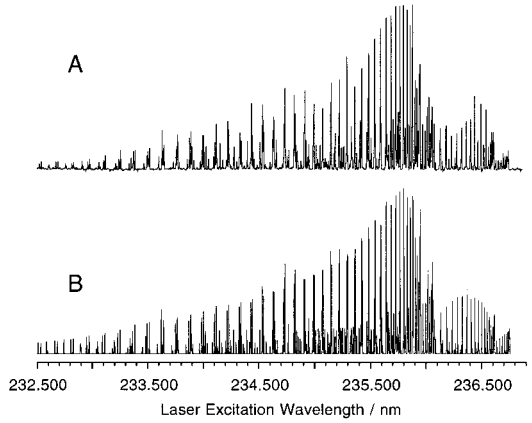

Figure 2. NO($^2\Sigma^+$, v'=0, $J' \leftarrow {}^2\Pi_\Omega$, $v'' = 1$, J'') from the Cl + ClNO reaction: (A) experimental spectrum; (B) simulated fine-structure spectrum. A 2:1 mixture of Cl_2/ClNO was photolyzed at 355 nm at a total pressure of 150 mTorr. The rotational distribution was parametrized using a Boltzmann function with a "temperature" of 950 K.

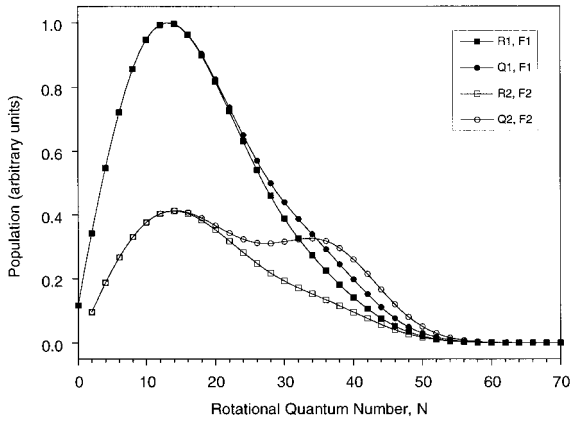

Figure 3. Rotational distributions for the main-branch R and Q transitions of NO($^2\Pi_\Omega$, $v'' = 1$), produced by the Cl + ClNO reaction, derived from the simulation presented in Figure 2B.

D. Observation of NO($v'' = 1$) from the Photofragmentation of $[ClNO]_n$ Clusters. The NO rotational distributions observed during the laser irradiation at 355 nm of a 5% mixture of ClNO diluted in He, expanded at backing pressures below 1 bar, are similar to the one presented in Figure 1, although the maximum is slightly shifted toward larger N values. As an example, the NO($v'' = 1$) rotational distributions obtained by working at a backing pressure of 1 bar are shown in Figure 4. We find the same Λ-doublet state and spin−orbit state preferences as in our photolysis studies of ClNO under bulk conditions (see Figure 1). This shows that still at 1 bar there is no significant ClNO clustering.

When the backing pressure of the mixture is increased to 3 bar, there appears a Boltzmann ensemble of NO($v'' = 1$) molecules described by a "temperature" of 310 ± 30 K and no spin−orbit preference, overlapped with the Gaussian distribution already assigned to the NO photofragment. This is the lowest backing pressure at which the Boltzmann component is observed. We derived the values of the rotational temperature and the spin−orbit populations from a spectral simulation, and the distributions are displayed in Figure 5. The Gaussian component

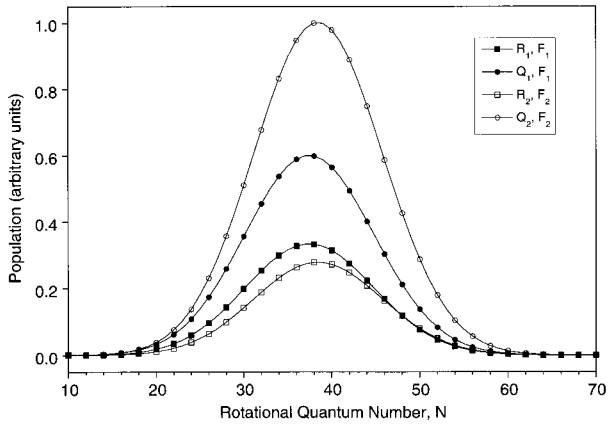

Figure 4. Rotational distributions for the main-branch R and Q transitions of NO($^2\Pi_\Omega$, $v'' = 1$) from the photofragmentation of jet-cooled ClNO monomers at 355 nm. A 3% mixture of ClNO diluted in He was expanded at a stagnation pressure of 1 bar.

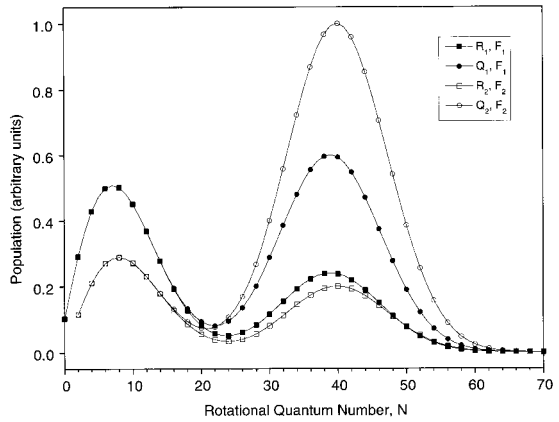

Figure 5. Rotational distributions for the main-branch R and Q transitions of NO($^2\Pi_\Omega$, $v'' = 1$), from the photolysis at 355 nm of a 3% mixture of ClNO diluted in He and expanded at a backing pressure of 3 bar.

has the same parameters as those employed in the simulation used to obtain Figure 4, which implies that the NO photofragment is being detected without undergoing collisional relaxation. This ensemble of NO molecules may originate from the photolysis of bare ClNO and/or NO molecules ejected from the surface of the clusters. Because the Boltzmann distribution was 310 K (i.e., close to room temperature), we carefully reduced as much as possible the length of the gas pulses, corroborated that the signal was observed only when the photolysis beam was entering the chamber, and adjusted a delay time of 50 ns between the photolysis and probe lasers. The lower NO rotational temperature observed under cluster conditions, as compared to 950 K observed from the Cl + ClNO reaction, as well as the absence of spin−orbit state preference, indicate that NO has been relaxed if the reaction is the source of this new ensemble of molecules.

The relative contribution of the NO($v'' = 1$) photofragment to the spectrum is drastically reduced upon increasing the backing pressure to 6 bar. However, the relaxation conditions in the jet environment are not strong enough to vibrationally relax NO($v'' = 1$). The spectral region close to the band heads was parametrized using a Boltzmann function with a "temperature" of 325 ± 35 K. Neither spin−orbit state nor Λ-doublet state preferences are observed under these conditions. Nitric oxide is not part of the $[ClNO]_n$ complexes during its detection because otherwise we should not be observing the NO($v'' = 1$) fine structure. Other spectra (not shown) were collected at

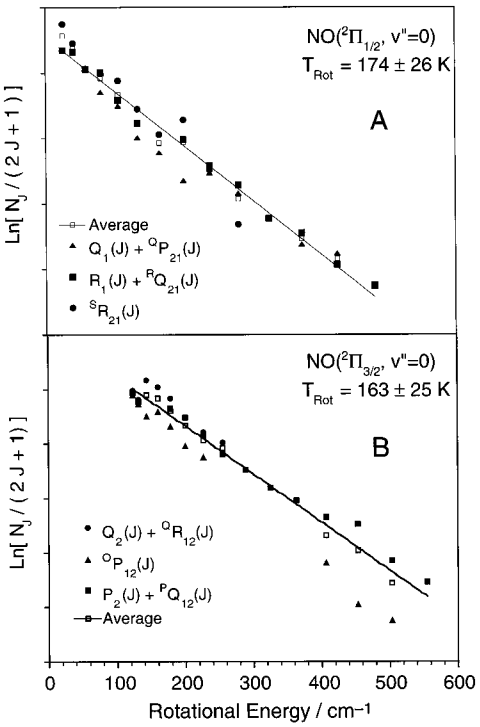

Figure 6. Boltzmann plots constructed from the integrated areas of rotational lines of NO in $v'' = 0$. A ClNO/He sample was expanded at a backing pressure of 3 bar and irradiated at 355 nm. (A) The "rotational temperature" was 174 ± 26 K for the F_1 spin−orbit state. (B) The "rotational temperature" was 163 ± 25 K for the F_2 spin−orbit state.

backing pressures ranging from 3 to 6 bar, showing a gradual relative reduction of the Gaussian component with respect to the Boltzmann one. An increase in the backing pressure translates into an increase in the average cluster size, which increases the probability of relaxation of the NO photofragment. Likewise, it should be more likely to observed the reaction upon increasing the backing pressures.

E. Observation of NO($v'' = 0$) from the Photofragmentation of $[ClNO]_n$ Clusters. The distribution of NO($v'' = 0$) rotational states from the irradiation of a sample expanded at a backing pressure of 3 bar was determined (1) from the spectral simulation of the NO experimental spectrum and (2) by integrating individual rotational lines. Only lines from different main branches with no overlap were considered and the integrated areas were corrected for line strength factors, although not for alignment effects. Following this approach we determined the "rotational temperatures" for the F_1 and F_2 manifolds to be 174 ± 26 and 163 ± 25 K, respectively (Figure 6). Using an average temperature of 170 K, we obtained excellent agreement between the simulated spectrum and the experimental spectrum. The rotational distributions of NO($v'' = 0$) obtained following these procedures are colder than that for NO($v'' = 1$) detected at the same backing pressure, and this implies that the former ensemble of molecules has been subjected to stronger relaxation conditions. The Boltzmann ensemble of NO molecules in $v'' = 0$ may originate from either or both of two sources: the fraction of ClNO parent molecules photolyzed in the interior of the clusters, where they can relax more effectively, and/or the Cl + ClNO reaction. While the reaction studied under bulk conditions exhibits strong spin−orbit state preference and a rotational temperature of 950 ± 100 K, the rotational temperature observed under cluster conditions is about 800 K lower, and the spin−orbit states are statistically populated. That is to say, if the reaction is contributing to the Boltzmann

component, then the NO product is being subjected to strong relaxation conditions.

Huber and co-workers observed NO bimodal distributions in their study of the photofragmentation of $[CH_3ONO]_n$ clusters as well as Ning and Pfab from the photofragmentation of HONO/water heterogeneous clusters.[20,22] Both groups assign the Boltzmann component to nitrous oxide photofragments that have been relaxed. In their experiments, the nascent distributions of the NO photofragment are Gaussian, as in our experiments, although there are no reactions that can produce NO. Thus, their findings stress the importance of considering relaxation processes within the cluster environments in our experiments.

F. Kinematic Analysis of the ClNO Photofragmentation. After the absorption of a photon by the ClNO molecule, the available energy to the Cl and NO products is $E_{avl} = E_{int}(ClNO) + h\nu - D_o(ClNO) = E_{so}(Cl) + E_{kin}(Cl) + E_{int}(NO) + E_{kin}(NO)$, where $E_{int}(ClNO)$ is the internal energy of ClNO (which may be neglected in studies of jet-cooled ClNO or approximated as the rotational energy of ClNO in gas-phase experiments at room temperature), $h\nu$ is the photon energy, $D_o(ClNO)$ is the dissociation energy of ClNO, $E_{kin}(Cl)$ and $E_{kin}(NO)$ are the corresponding kinetic energies of the Cl and NO fragments, $E_{so}(Cl)$ is the spin−orbit energy of the $Cl(^2P_{1/2})$ atom (preferentially formed during the photofragmentation of ClNO at 355 nm), and $E_{int}(NO)$ is the internal energy of NO. Conservation of linear momentum in the center-of-mass relates $E_{kin}(Cl)$ to $E_{kin}(NO)$, while spectroscopically one can scan individual vibro-rotational states of NO and assign $E_{int}(NO)$. It follows that for a given set of quantum numbers, the NO velocity is uniquely determined,

$$v_{NO}(F_i, v'', J'') = \sqrt{\frac{2(E_{av1} - E_{int}(NO))}{m_{NO}(1 + m_{NO}/m_{Cl})}} \qquad (7)$$

where m_{NO} and m_{Cl} are the atomic masses of the specified species. Once the velocity of the NO photofragment has been calculated, the Doppler width is readily estimated using eq 8 for a rotational line,

$$\Delta\tilde{\nu}_{Doppler} = 2\tilde{\nu}_o \frac{v_{NO}(F_i, v'', J'')}{c} \qquad (8)$$

where $\Delta\tilde{\nu}_{Doppler}$ is the fwhm of the rotational line, c is the speed of light, and $\tilde{\nu}_o$ is the center frequency. For Gaussian-shaped lines, the Doppler width is obtained by knowing the laser bandwidth, $\Delta\tilde{\nu}_{Doppler}^2 = \Delta\tilde{\nu}_{Exp}^2 - \Delta\tilde{\nu}_{Laser}^2$, where $\Delta\tilde{\nu}_{Exp}$ is the experimental fwhm of the lines. Because $\Delta\tilde{\nu}_{Laser}$ is 0.04 cm^{-1} for our dye laser system, the correction due to $\Delta\tilde{\nu}_{Laser}$ to the Doppler widths is very small. Employing eq 8, we can estimate a fwhm of 0.39 cm^{-1} for the $NO(^2\Pi_{3/2}, v'' = 1, J'' = 38.5)$ vibro-rotational state, where the center frequency is 42 624 cm^{-1}.

G. Translational Energy Measurements. Both the photolysis of ClNO at 355 nm and the Cl + ClNO reaction produce $NO(v'' = 0, 1)$ and the information provided so far is not sufficient to conclude whether the Cl + ClNO reaction is taking place within the $[ClNO]_n$ clusters. Fortunately, Doppler spectroscopy enabled us to measure the translational energy of NO, allowing us to identify the different processes occurring within the cluster.

Figure 7A displays part of the NO spectrum from the photolysis of a 1:1 mixture of Cl_2:ClNO photolyzed under bulk conditions at a total pressure of 150 mTorr. In this experiment NO is observed simultaneously from the Cl + ClNO reaction and from the ClNO photodissociation. Qualitatively, the $P_1(36.5)$ line is wider than the $R_1(23.5) + {}^SR_{21}(18.5)$ line because the former probes the ClNO photofragmentation, whereas the latter probes the NO reaction product. On the other hand, parts B−E of Figure 7 display NO spectra recorded under jet conditions, increasing the backing pressure from 1.7 to 4.4 bar. Figure 7B corresponds to the photodissociation of ClNO with no significant clustering. Since the $P_1(36.5)$ line probes the fragmentation process almost exclusively, the spectra depicted in Figure 7C−E have been normalized with respect to it. It is noted that the intensity of the $R_1(23.5) + {}^SR_{21}(18.5)$ line increases upon increasing the backing pressure because the Cl + ClNO reaction and relaxation processes are taking place. It is also noted that the $P_2(38.5) + {}^PQ_{12}(38.5)$ line is subjected to a relaxation process, although it probes the photofragmentation process.

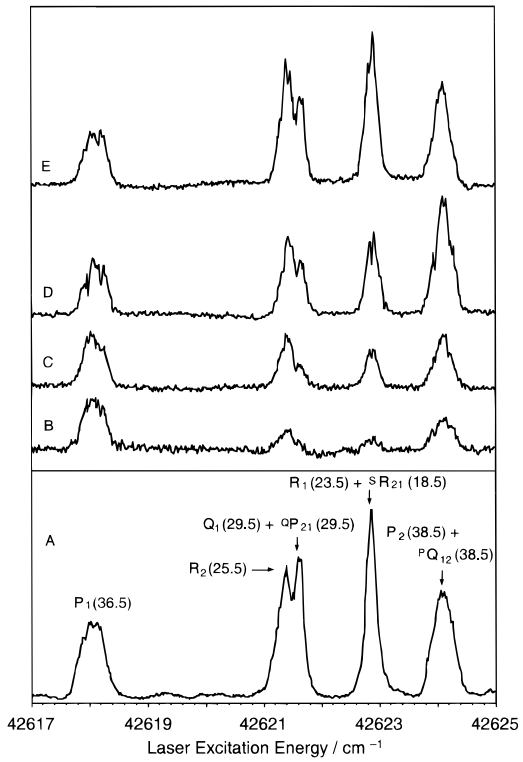

Figure 7. (A) NO spectrum from the photolysis of a 1:1 mixture of Cl_2:ClNO photolyzed under bulk conditions at a pressure of 150 mTorr. The Cl + ClNO reaction and the ClNO photodissociation are observed simultaneously. Figures B−E display NO spectra recorded under jet conditions, at the following backing pressures: (B) 1.7 bar, (C) 2.3 bar, (D) 3.0 bar, and (E) 4.4 bar. Spectrum B corresponds to the photodissociation of ClNO with no significant clustering. The relative intensity of the $R_1(23.5) + {}^SR_{21}(18.5)$ line increases upon increasing the backing pressure because the Cl + ClNO reaction and relaxation processes are simultaneously taking place.

Figure 8A displays the Doppler profile of the $R_1(23.5) + {}^SR_{21}(18.5)$ line recorded under the conditions specified in Figure 7A; namely, both the reaction and the photofragmentation process are being observed simultaneously in the gas phase. This line has been fitted by adding two Gaussian functions centered at 42 623 cm^{-1}: $c_1G_1 + c_2G_2$, with $c_1 = 0.70$ and $\Delta\tilde{\nu}_1 = 0.17$ cm^{-1}, and $c_2 = 0.30$ and $\Delta\tilde{\nu}_2 = 0.38$ cm^{-1}. That is to say, this lines appears in a region of the spectrum in which both rotational distributions overlap. As a result of the particular conditions of this experiment, there is 40% more contribution from the reaction to this line.

The $P_2(38.5) + {}^PQ_{12}(38.5)$ line is depicted in Figure 8B, with fwhm of 0.38 cm^{-1}, recorded during the photolysis of 150 mTorr of ClNO. This line probes the $NO(^2\Pi_{3/2}, v'' = 1, J'' = 38.5)$

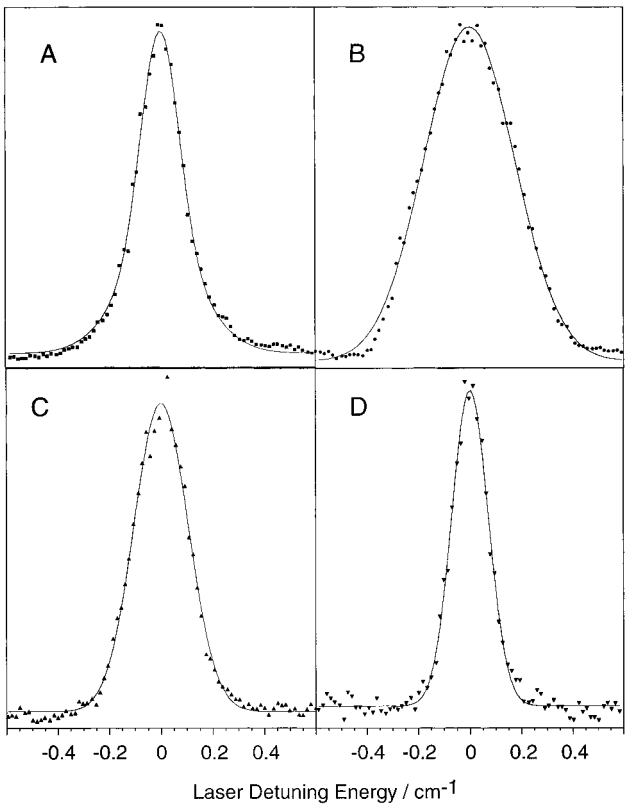

Figure 8. (A) Doppler profile of the $R_1(23.5) + {}^SR_{21}(18.5)$ line recorded under the conditions specified in Figure 7A. This line has been fitted by adding two Gaussian functions centered at 42 623 cm^{-1}: $c_1G_1 + c_2G_2$, with $c_1 = 0.70$ and $\Delta\tilde{\nu}_1 = 0.17$ cm^{-1} and $c_2 = 0.30$ and $\Delta\tilde{\nu}_2 = 0.38$ cm^{-1}. (B) The $P_2(38.5) + {}^PQ_{12}(38.5)$ line with fwhm of 0.38 cm^{-1}, recorded during the photolysis of 150 mTorr of ClNO. The Doppler width of this line allows one to calculate the (lab frame) velocity of the photofragment to be 1336 m/s. (C) The $R_1(23.5) + {}^SR_{12}(18.5)$ line (fwhm = 0.24 cm^{-1}, and $\nu_o = 42623$ cm^{-1}) detected at a backing pressure of 3 bar. Its Doppler profile is Gaussian and probes a Maxwell−Boltzmann distribution of velocities to which can be associated a translational temperature $T_{trans} \approx 1855$ K, a mean velocity, and a mean kinetic energy of 1144 m/s and 1640 cm^{-1}, respectively. (D) The NO reaction product probed by the $R_2(8.5)$ line (fwhm = 0.18 and $\tilde{\nu}_o = 42\,445$ cm^{-1}) with a "translational temperature" of 1052 K and a (lab frame) mean velocity of 862 m/s. The width and Doppler profile of this line are the same regardless whether this line probes the photolysis of a sample of ClNO expanded at a backing pressure of 3 bar or the Cl + ClNO reaction under bulk conditions.

vibro-rotational state for which we previously calculated a Doppler width of 0.39 cm^{-1} using eqs 7 and 8. The excellent agreement between the measured and the estimated line widths confirms that the NO photofragment is not undergoing a significant translational relaxation under these experimental conditions. Moreover, the Doppler width of this line allows one to calculate the (lab frame) velocity of the photofragment to be 1336 m/s.

A closer examination to the $R_1(23.5) + {}^SR_{12}(18.5)$ line (fwhm = 0.24 cm^{-1}, and $\tilde{\nu}_o = 42\,623$ cm^{-1}) is given in Figure 8C, which was detected at a backing pressure of 3 bar. Its Doppler profile is Gaussian, and this line represents a Maxwell−Boltzmann distribution of velocities to which a translational temperature can be associated,[46]

$$T_{trans} = \left(\frac{\Delta\tilde{\nu}c}{2\tilde{\nu}_o}\right)^2 \frac{m_{NO}}{2k_B \ln 2} \qquad (9)$$

where k_B is the Boltzmann constant. Using eq 9 for the $R_1(23.5) + {}^SR_{12}(18.5)$ line we obtain $T_{trans} \approx 1855$ K, which allows us to calculate the mean velocity and the mean kinetic energy to be 1144 m/s and 1640 cm^{-1}, respectively.

The width and Doppler profile of the $R_2(8.5)$ line (Figure 8D) are the same regardless of whether this line probes the photolysis of a sample of ClNO expanded at a backing pressure of 3 bar or the Cl + ClNO reaction under bulk conditions. This observation then supports the possibility that the reaction is occurring within the clusters. For the NO reaction product probed by the $R_2(8.5)$ line (fwhm = 0.18 and $\tilde{\nu}_o = 42\,445$ cm^{-1}) a "translational temperature" of 1052 K may be calculated by using eq 9, together with a (lab frame) mean velocity of 862 m/s.

H. Energy Disposed into Cl_2 Reaction Product. The photodissociation of Cl_2 at 355 nm is our source of $Cl(^2P_{3/2})$ atoms ($\beta = -1$).[47] The excess energy, given by $E_{exc} = h\nu + E_{int}(Cl_2) - D_o(Cl_2)$, can be estimated to be 8170 cm^{-1} if the internal energy of Cl_2 is neglected (which is mostly rotational at room temperature). It follows that the velocity of the Cl atoms in the center-of-mass frame is $w_{Cl} = 1659$ m/s.

The available energy for the Cl + ClNO reaction is given by

$$\begin{aligned} E_{avl} &= \Delta H^\circ + E_{coll} + E_{int}(ClNO) \\ &= E_{int}(NO) + E_{int}(Cl_2) + E_{trans}(NO) + E_{trans}(Cl_2) \end{aligned} \qquad (10)$$

where $\Delta H^\circ = -6982$ cm^{-1} is the enthalpy of the reaction, E_{coll} is the collision energy, and E_{int} and E_{trans} denote the internal energies and translational energies of the indicated species, respectively. Although the collision energy is given by

$$E_{coll} = \frac{1}{2}m(w_{Cl}{}^2 + v_{Cl_2}{}^2 + v_{ClNO}{}^2) \qquad (11)$$

it may be approximated as $(\mu w_{Cl}{}^2)/2 \approx 2780$ cm^{-1} (33.2 kJ/mol), where μ is the reduced mass of the Cl and ClNO reactants. An estimate of $E_{int}(ClNO)$ of 310 cm^{-1} is obtained by assuming that most of the ClNO internal energy is rotational. Therefore, the energy available to the reaction amounts to 10 072 cm^{-1}.

The thermal distribution of internal states of the Cl_2 molecule (the Cl atom source) introduces considerable smearing into the translational energy distribution of the Cl atoms, which is described by a Gaussian function with a fwhm given by[48−50]

$$\delta E_{coll} = \sqrt{\frac{4m_{ClNO}(2m_{Cl} + m_{ClNO})}{(m_{Cl} + m_{ClNO})^2} RTE_{exc} \ln 2} \qquad (12)$$

For the Cl + ClNO reaction δE_{coll} equals 2723 cm^{-1} (32.6 kJ/mol), which means that in our experiments δE_{coll} and E_{coll} are of the same magnitude.

We now seek to calculate the internal energy of the Cl_2 (unobserved) product that correlates with a given vibro-rotational state of NO. This can be done employing eq 10. The NO velocity (v_{NO}) in the lab frame is related to the center-of-mass velocity, V_{cm}, and w_{NO} by the equation $v_{NO} = V_{cm} + w_{NO}$. In the present case, $V_{cm} \approx m_{Cl}/(m_{Cl} + m_{ClNO})v_{Cl}$ amounts to 530 m/s. Assuming that the ClNO target molecule is initially stationary in the center-of-mass coordinate, the velocity of NO in the lab frame is then related to V_{cm} and w_{NO} by the cosine law $v_{NO}{}^2 = V_{cm}{}^2 + w_{NO}{}^2 + V_{cm}w_{NO}\cos\theta$, where θ is center-of-mass scattering angle of NO. Since we did not observe vector correlations between V_{cm} and w_{NO} in our high-resolution experiments (the Doppler profiles were Gaussian), the average velocity of NO in the center-of-mass frame is $\langle w_{NO}{}^2\rangle = \langle v_{NO}{}^2\rangle - \langle V_{cm}{}^2\rangle$. Because in section F we found $v_{NO} = 862$ m/s, we

can calculate w_{NO} and $E_{trans}(NO)$ to be 679 m/s and 579 cm^{-1}, respectively. The translational energy of the Cl_2 product is ($m_{NO}/2m_{Cl}$) times the kinetic energy of NO, that is, $E_{trans}(Cl_2) = 245$ cm^{-1}. Thus, the fraction of the total available energy which is channeled into product relative translation is $f_{trans} = 0.08$.

In section C we calculated $E_{rot}(NO) \approx 660$ cm^{-1} ($f_{rot}(NO) \approx 0.06$). In the present experiments we are detecting NO($v'' = 1$), with $E_{vib}(NO) \approx 2825$ cm^{-1}. The internal energy disposed into the Cl_2 product may be estimated by eq 10 to be 5761 cm^{-1}. In other words, the Cl_2 (unobserved) fragment formed in coincidence with the spectroscopically selected NO($v'' = 1$) molecule may be formed up to $v' = 10$, although not electronically excited, and $f_{int}(Cl_2) \approx 0.57$.

The question now is, how is this energy being distributed between the rotational and vibrational degrees of freedoms of Cl_2? Burn and Dainton measured a very small activation energy (≈4 kJ/mol) for this reaction and determined that the potential energy surface is attractive.[42] On the basis of Burn and Dainton's findings, the fact that more than 50% of the available energy becomes $E_{int}(Cl_2)$, and the modest rotational excitation observed in the NO product, one could anticipate low Cl_2 rotational excitation and argue that the Cl + ClNO reaction proceeds through a direct atom abstraction mechanism.[42,51]

Another equation is needed to know the answer to this question and we should consider the angular momentum conservation for this reaction, as it dictates how the rotational energy is distributed between the products: $\mathbf{L}_{Cl} + \mathbf{J}_{ClNO} + \mathbf{L} = \mathbf{J}_{NO} + \mathbf{J}_{Cl_2} + \mathbf{L}'$, where $\mathbf{L}_{Cl}$ denotes the orbital angular momentum of the Cl atom, **J** are the rotational angular momenta of the indicated species, and **L** and **L′** are the orbital angular momenta of the reactants and of the product, respectively. An average impact parameter, $b \approx 10^{-9}$ m, was estimated from the available rate constant,[43] assuming that for the present experiments it holds the condition, $k \approx v_{Cl}\pi b^2$. It follows that the orbital angular momentum in the entrance channel, $\mathbf{L} = \mu v_{Cl} b \approx 100\hbar$, is the largest source of angular momentum for the reaction. Although we measured $\mathbf{J}_{NO}$ experimentally, $\mathbf{J}_{Cl_2} + \mathbf{L}'$ are still unresolved. We indeed know that 8% of E_{avl} appears as translational energy of the product. It follows that the relative product velocity (v') is small and its contribution to the exit channel orbital angular momentum should be small as well: $\mathbf{L}' = \mu' b' v'$, where μ' and b' are the reduced mass of the Cl_2 and NO product and the exit channel impact parameter, respectively. Thus, it is still necessary to know b' and the geometry of the Cl−ClNO reaction complex in order to estimate $\mathbf{J}_{Cl_2}$.

I. Spin−Orbit Effects. As we already mentioned, the relative population of the spin−orbit states is $F_1/F_2 = 2.5$ for the reaction. It should be noted that the spin−orbit splitting constant of NO is 123 cm^{-1}, which is 1% of the total available energy. Therefore, a statistical population of the spin−orbit states should be close to unity and clearly the reaction is producing NO($^2\Pi_{1/2}$, N″) with a market preference. We are actually observing the reaction involving the lowest energy spin−orbit states, Cl($^2P_{3/2}$) + ClNO → Cl_2 + NO($^2\Pi_{1/2}$). This indicates that the reaction follows an adiabatic trajectory and there are no long-range interactions that can cause transitions between the $^2\Pi_{1/2}$ and $^2\Pi_{3/2}$ states in the exit channel. Actually, the time τ required to observe transitions between two adiabatic states is $\hbar/\Delta V = 14$ fs, where ΔV in the present case is the spin−orbit splitting between the two surfaces correlating with the $^2\Pi_{1/2}$ and $^2\Pi_{3/2}$ states.[52] Since we calculated the velocity of NO in the center-of-mass to be 679 m/s, we can estimate that during the time τ the NO reaction product is 28 Å away from the center-of-mass, which is too far to be subjected to fine-structure mixing. Thus, our observations are consistent with this model.

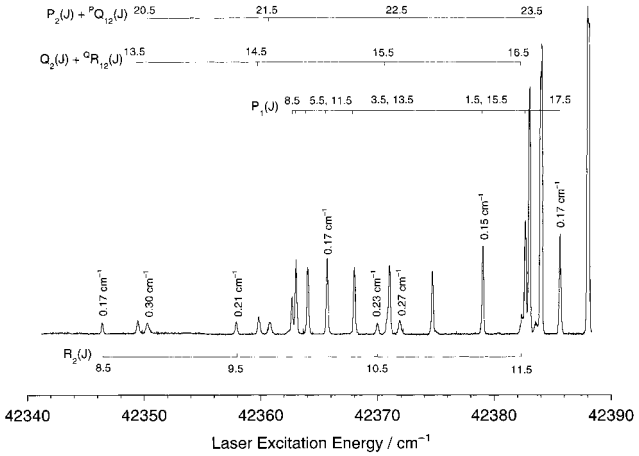

Figure 9. High-resolution laser excitation spectrum of low rotational states of NO($v'' = 1$) from the photofragmentation of the $[ClNO]_n$ clusters. A ClNO/He sample was expanded at a backing pressure of 3 bar. The fwhm of the rotational lines belonging to the P_1 branch are narrow. In contrast, the widths of the rotational lines that probe the F_2 manifold increase with the J quantum number, which means that the cross sections for relaxation within the F_2 manifold are larger than those for the F_1 manifold.

J. Doppler Scans of Low Rotational States of NO($v'' = 1$) from the $[ClNO]_n$ Photofragmentation. A high-resolution laser excitation spectrum of NO($v'' = 1$) from the photofragmentation of the $[ClNO]_n$ clusters is presented in Figure 9. A ClNO/He sample was expanded at a backing pressure of 3 bar. The fwhm of the $P_1(1.5)$ line is 0.15 cm^{-1}, and this value remains essentially unchanged in this branch up to the $P_1(17.5)$ line. In contrast, the widths of the rotational lines that probe the F_2 manifold increase with the J quantum number. For example, the fwhm of the $R_2(8.5)$ line is 0.17 cm^{-1}, whereas the fwhm of the $R_2(10.5)$ and $P_2(20.5) + {}^PQ_{12}(20.5)$ lines are 0.23 and 0.30 cm^{-1}, respectively. The preferential broadening of the rotational lines corresponding to high rotational states may be explained as follows. The NO photofragments are produced (with larger probability) in high rotational states and with a large translational energy. However, as a result of the interactions within the clusters, part of the rotational and translational energy is transferred, and this happens more efficiently to levels closer in energy. These relaxed states are then observed as the tail of the Boltzmann ensemble of nitric oxide molecules. Moreover, since the lower rotational lines of NO in the F_1 manifold recorded under cluster conditions are not undergoing a systematic broadening, they do not probe the relaxed NO photofragment and must belong to the NO reaction product.

From Figure 4 we observe that the NO photofragment is preferentially formed in the F_2 manifold in the antisymmetric Λ-doublet state, as probed by the Q-branch. On the other hand, Figure 9 shows that both the symmetric and antisymmetric Λ-doublet states of the F_2 manifold are broadened, as probed by the R_2 and $Q_2 + {}^QR_{12}$ branches, respectively. Therefore, a propensity rule to conserve the symmetry of Λ-doublet states is not observed. Because the lower rotational states in the F_1 manifold are not broadened, this implies that the population transfer from the F_2 manifold to the F_1 manifold is less efficient than the relaxation within the F_2 manifold.

Our results are in qualitative agreement in two aspects with the theoretical work of Orlikowski and Alexander on the NO-($^2\Pi$) + Ar system.[53] First, these authors found that the cross

sections for inelastic collisional transitions involving rotational levels that belong to different manifolds are smaller than those for transitions within a manifold. This first point is consistent with the results displayed in Figure 9, in the sense that we observe intramultiplet relaxation in the F_2 manifold. Second, they predicted that for transitions between specified values of J and J' within a manifold, the cross section for ϵ-changing transitions are larger for the F_2 manifold. In our experiment we do not have state-to-state resolution to rigorously confirm this rule, but on the basis of the systematic broadening observed for the R_2, $P_2 + {}^PQ_{12}$, and $Q_2 + {}^QR_{12}$ branches, it is clear that the cross sections for relaxation within the F_2 manifold are larger than those for F_1.

IV. Summary

The photofragmentation of ClNO at 355 nm produces NO in $v'' = 1$ with a small spin−orbit preference of $F_1/F_2 = 1.2$, but with Λ-doublet state preferences of $\Pi(A'')/\Pi(A'') = 2.0$ and 4.0 for the F_1 and F_2 manifolds, respectively. The distribution of rotational states was parametrized using a Gaussian function centered at $N = 34$, with a fwhm of 17. The fwhm of the rotational lines of the NO photofragment is ≈ 0.38 cm^{-1}, corresponding to a kinetic energy of 2240 cm^{-1}.

The Cl + ClNO reaction was studied under bulk conditions at a collision energy of 2780 cm^{-1}, and the total available energy was 10 070 cm^{-1}. The distribution of rotational states for the $v'' = 1$ level of NO is described by a Boltzmann function with a temperature of 950 ± 100 K, corresponding to an average rotational energy of 660 cm^{-1}. The relative population of the spin−orbit states was $F_1/F_2 = 2.5$, with a small Λ-doublet state preference of $\Pi(A'')/\Pi(A') = 1.2$. A fwhm of 0.18 cm^{-1} was measured for the NO rotational lines, corresponding to a translational temperature of 1052 K, and a (center-of-mass) velocity and translational energy of 679 m/s and 578 cm^{-1}, respectively. The Cl + ClNO reaction proceeds through a direct atom abstraction mechanism and 57% of the total available energy is channeled into the Cl_2 internal degrees of freedom. Only 8% of E_{avl} is disposed into the product relative translational energy.

During the irradiation of the $[ClNO]_n$ clusters at 355 nm, a Boltzmann ensemble of NO($v'' = 1$) molecules described by a "temperature" of 310 ± 30 K with no spin−orbit or Λ-doublet preferences is observed, overlapped with the Gaussian distribution already assigned to the NO photofragment. The Gaussian ensemble of NO molecules may originate from the photolysis of bare ClNO and/or NO molecules ejected from the surface of the clusters. While the relative contribution of the NO($v'' = 1$) photofragment to the spectrum is drastically reduced upon increasing the backing pressure, the relaxation conditions in the jet environment are not strong enough to vibrationally relax NO($v'' = 1$). Nitric oxide is not part of the $[ClNO]_n$ complexes during its detection. The distribution of NO($v'' = 0$) rotational states was Boltzmann with "rotational temperatures" for the F_1 and F_2 manifolds of 174 ± 26 and 163 ± 25 K, respectively. The Boltzmann ensemble of NO molecules in $v'' = 0$ may originate from either or both of two sources: the fraction of ClNO parent molecules photolyzed in the interior of the clusters, where they can relax more effectively, and/or the Cl + ClNO reaction. During the photofragmentation of the clusters, the NO photofragment is translationally and rotationally relaxed. Our high-resolution experiments provide evidence that supports that the Cl + ClNO reaction is taking place in the environment of the clusters. We find that the relative cross sections for inelastic collisional transitions between rotational levels which belong to different manifolds are smaller than those for transitions within a manifold and that the cross sections for relaxation within the F_2 manifold are larger than those for F_1, and these results are in qualitative agreement with theory.[53]

Acknowledgment. The financial support for this work from the U.S. Department of Energy EPSCoR Program, by Fondos Institucionales de la Universidad de Puerto Rico, and by the NIH-MBRS Program, is gratefully acknowledged. The excimer laser was purchased with funds of the Puerto Rico Laser Facility, under the auspices of the RCMI Program and NSF-EPSCoR. C.C. is grateful for the award of a GAANN fellowship. The authors wish to thank Ruth Molina for the design of some parts of the molecular beam chamber, Rudy Rivera for the construction of several parts of the molecular beam machine, and Michael Joyner for the construction of a circuit to operate the pulsed solenoid valve.

References and Notes

(1) Castleman, A. W., Jr.; Bowen, K. H., Jr. *J. Phys. Chem.* **1996**, *100*, 12911. Echt, O.; Dao, P. D. Morgan, S.; Castleman, A. W., Jr. *J. Chem. Phys.* **1985**, *82*, 4076. Stephan, K.; Futrell, J. H.; Peterson, K. I.; Castleman, A. W., Jr.; Mark, T. D. *J. Chem. Phys.* **1982**, *72*, 2408.

(2) *Chemical Reactions in Clusters*; Bernstein, E. R., Ed.; Oxford University: New York, 1996. Gerber, R. B.; McCoy, A. B.; García-Vela, A. *Annu. Rev. Phys. Chem.* **1994**, *45*, 275.

(3) Schröder, T.; Schinke, R.; Liu, S.; Bacic, Z.; Moskowitz, J. W. *J. Chem. Phys.* **1995**, *103*, 9228.

(4) Finney, L. M.; Martens, C. C. *J. Phys. Chem.* **1993**, *97*, 13477.

(5) **.** Droz, T.; Knochenmuss, R.; Leutwyler, S. *J. Chem. Phys.* **1990**, *93*, 4520. Knochenmuss, R.; Leutwyler, S. J. *J. Chem. Phys.* **1989**, *91*, 1268. Knochenmuss, R.; Cheshnovsky, O.; Leutwyler, S. *Chem. Phys. Lett.* **1988**, *144*, 317.

(6) Cohen, R. C.; Saykally, R. J. *J. Phys. Chem.* **1992**, *96*, 1024. Bacic, Z.; Miller, R. E. *J. Phys. Chem.* **1996**, *100*, 12945. Willey, K. F.; LaiHing, K.; Taylor, T. G.; Duncan, M. A. *J. Phys. Chem.* **1996**, *97*, 7435.

(7) *Chem. Rev.* **1994**, *94* (issue of van der Waals Molecules), 1721. Buck, U. *J. Phys. Chem.* **1988**, *92*, 1023. Nesbitt, D. J. *Chem. Rev.* **1988**, *88*, 843.

(8) Shin, S. K.; Chen, Y.; Nickolaisen, S.; Sharpe, S. W.; Beaudet, R. A.; Wittig, C. *Adv. Photochem.* **1991**, *16*, 249. Buelow, S.; Noble, M.; Radhakrishnan, G.; Reisler, H.; Wittig, C. *J. Phys. Chem.* **1986**, *90*, 1015.

(9) King, D. S.; Sauder, D. G.; Casassa, M. P. *J. Chem. Phys.* **1992**, *97*, 5919. King, D. S.; Sauder, D. G.; Casassa, M. P. *J. Chem. Phys.* **1994**, *100*, 4200.

(10) Breckenridge, W. E. *Acc. Chem. Res.* **1989**, *22*, 21.

(11) Duval, M. C.; Soep, B.; Breckenridge, W. E. *J. Phys. Chem.* **1991**, *95*, 7153.

(12) Shorter, J. H.; Casassa, M. P.; King, D. S. *J. Chem. Phys.* **1988**, *88*, 4739.

(13) Honma, K.; Fujimura, Y.; Kajimoto, O.; Inoue, G. *J. Chem. Phys.* **1988**, *88*, 4739. Bai, Y. Y.; Ogai, A.; Qian, C. X. W.; Iwata, L.; Segal, G. A.; Reisler, H. *J. Phys. Chem.* **1995**, *99*, 15573.

(14) Levy, D. H. *Adv. Chem. Phys.* **1981**, *47*, 323.

(15) Ewing, G. E. *J. Phys. Chem.* **1987**, *91*, 4662.

(16) Drobits, J. C.; Skene, J. M.; Lester, M. I. *J. Chem. Phys.* **1986**, *84*, 2896.

(17) Cline, J. I.; Sivakumar, N.; Evard, D. D.; Bieler, C. R.; Reid, B. P.; Halberstadt, N.; Hiar, S. R.; Janda, K. C. *J. Chem. Phys.* **1989**, *90*, 2605. Butz, K. W.; Catlett, D. L.; Ewing, G. E.; Krajnovich, D.; Parmenter, C. S. *J. Phys. Chem.* **1986**, *90*, 3533.

(18) Garvey, J. F.; Bernstein, R. B. *J. Am. Chem. Soc.* **1986**, *108*, 6096. Garvey, J. F.; Bernstein, R. B. *J. Phys. Chem.* **1986**, *90*, 3577. Garvey, J. F.; Bernstein, R. B. *Chem. Phys. Lett.* **1986**, *126*, 394.

(19) Sivakumar, N.; Burak, I.; Cheung, W.-Y.; Houston, P. L.; Hepburn, J. W. *J. Phys. Chem.* **1995**, *89*, 3609. Sivakumar, N.; Hall, G. E.; Houston, P. L.; Hepburn, J. W.; Burak, I. *J. Chem. Phys.* **1988**, *88*, 3692.

(20) (a) Bergmann, K.; Huber, J. R. *J. Phys. Chem. A* **1997**, *101*, 259. (b) Kades, E.; Rösslein, U.; Brühlmann, U.; Huber, J. R. *J. Phys. Chem.* **1993**, *97*, 989.

(21) Jones, A. B.; Lopez-Martens, R.; Stace, A. J. *J. Phys. Chem.* **1995**, *99*, 6333.

(22) Ning, C. L.; Pfab, J. *J. Phys. Chem. A* **1997**, *101*, 6008.

(23) Rudich, Y.; Hurwitz, Y.; Lifson, S.; Naaman, R. *J. Chem. Phys.* **1993**, *98*, 2936.

(24) Langridge-Smith, P. R. R.; Carrasquillo, E.; Levy, D. H. *J. Chem. Phys.* **1981**, *74*, 6513.

(25) Huber, K. P.; Herzberg, G. *Molecular Spectra and Molecular Structure, IV. Constants of Diatomic Molecules*; Van Nostrand Reinhold: New York, 1979. Herzerg, G. *Spectra of Diatomic Mol*ecules; Van Nostrand Reinhold: New York, 1950; p 222.

(26) Schleicher, D. G.; A'Hearn, M. F. *Astrophys. J.* **1982**, *258*, 864.

(27) Bai, Y. Y.; Ogai, A.; Qian, C. X. W.; Iwata, L.; Segal, G. A.; Reisler, H. *J. Chem. Phys.* **1989**, *90*, 3903.

(28) Vegiri, A.; Alexander, M. H. *J. Chem. Phys.* **1994**, *101*, 4722. Schinke, R.; Nonella, M.; Suter, H. U.; Huber, J. R. *J. Chem. Phys*. **1990**, *93*, 1098.

(29) Roehl, C. M.; Orlando, J. J.; Calvert, J. G. *J. Photochem. Photobiol. A.: Chem*. **1992**, *69*, 1.

(30) Calvert, J. G.; Pitts, J. N. *Photochemistry*; John Wiley and Sons: New York, 1966; p 230.

(31) Chichinin, A. I. *Chem. Phys. Lett*. **1993**, *209*, 459.

(32) Tictin, A.; Bruno, A. E.; Brühlmann, U.; Huber, J. R. *Chem. Phys.* **1988**, *125*, 403.

(33) Bruno, Y. Y.; Bruhlmann, U.; Huber, J. R. *Chem. Phys.* **1988**, *120*, 155.

(34) Skorokhodov, V.; Sato, Y.; Suto, K.; Matsumi, Y.; Kawasaki, M. *J. Phys. Chem*. **1996**, *100*, 12321.

(35) Busch, G. E.; Wilson, K. R. *J. Chem. Phys*. **1972**, *56*, 3655.

(36) Qian, C. X. W.; Ogai, A.; Iwata, L.; Reisler, H. *J. Chem. Phys.* **1990**, *92*, 4296. Qian, C. X. W.; Ogai, A.; Brandon, J.; Bai, Y.; Reisler, H. *J. Phys. Chem.* **1991**, *95*, 6763.

(37) Hall, G. E.; Sivakumar, N.; Chawla, D.; Houston, J. W.; Burak, I. *J. Chem*. *Phys.* **1988**, *88*, 3682.

(38) Greene, C. H.; Zare, R. N. *J. Chem. Phys*. **1983**, *78*, 6741. Case, D. A.; McClelland, G. M.; Herschbach, D. R. *Mol. Phys*. **1978**, *35*, 541. Ashfold, M. N. R.; Lambert, I. R.; Mordaunt, D. H.; Morley, G. P.; Western, C. M. *J. Phys. Chem.* **1992**, *96*, 2938. Dixon, R. N. *J. Chem. Phys*. **1986**, *85*, 1866. Zare, R. N. *Angular Momentum*; Wiley: New York, 1988; p 314. Orr-Ewing, A. J.; Zare, R. N. In *The Chemical Dynamics and Kinetics of Small Radical*, Liu, K., Wagner, A., Eds.; World Scientific: Singapore, 1995; Vol. 2, p 936. Dagdigian, P. J. In *Atomic and Molecular Beam Methods;* Scoles, G., Ed.; Oxford University: New York, 1988; Vol. 1, p 596.

(39) Alexander, M. H.; Andresen, P.; Bacis, R.; Bersohn, R.; Comes, F. J.; Dagdigian, P. J.; Dixon, R. N.; Field, R. W.; Flynn, G. W.; Gericke, K.-H.; Grant, E. R. Howard, B. J.; Huber, J. R.; King, D. S.; Kinsey, J. L.; Kleinermanns, K.; Kuchitsu, K.; Luntz, A. C.; McCaffery, A. J.; Pouilly, B.; Reisler, H.; Rosenwaks, S.; Rothe, E. W.; Shapiro, M.; Simons, J. P.; Vasudev, R.; Weisenfeld, J. R.; Wittig, C.; Zare, R. N. *J. Chem. Phys*. **1988**, *89*, 1749.

(40) Andresen, P.; Ondrey, G. S.; Titze, V.; Rothe, E. W. *J. Chem. Phys.* **1984**, *80*, 2548.

(41) Basco, N.; Norrish, R. G. W. *Proc. R. Soc. A* **1962**, *268*, 291.

(42) Burns, W. G.; Dainton, F. S. *Trans. Faraday Soc*. **1952**, *48*, 52.

(43) Grimley, A. J.; Houston, P. L. *J. Chem. Phys.* **1980**, *72*, 1471.

(44) Clyne, M. A. A.; Cruse, H. W.; Watson, R. T. *J. Chem. Soc., Faraday Trans. 2* **1972**, *68*, 153.

(45) Moser, M. D.; Weitz, E.; Schatz, G. C. *J. Chem. Phys.* **1983**, *78*, 757.

(46) Trentelman, K. A.; Kable, S. H.; Moss, D. B.; Houston, P. L. *J. Chem. Phys*. **1989**, *91*, 7498.

(47) Matsumi, Y.; Tonokura, K.; Kawasaki, M. *J. Chem. Phys*. **1992**, *97*, 1065.

(48) Chantry, P. J. *J. Chem. Phys*. **1971**, *55*, 2746.

(49) Bernstein, R. B. *Comments At. Mol. Phys*. **1973**, *4*, 43.

(50) van der Zande, W. J.; Zhang, R.; Zare, R. N. *J. Chem. Phys*. **1991**, 95, 8205.

(51) Levine, R. D.; Bersntein, R. B. *Molecular Reaction Dynamics and Chemical Reactivity*; Oxford University Press: New York, 1987.

(52) Graff, M. M.; Wagner, A. F. *J. Chem. Phys*. **1990**, *92*, 2423.

(53) Orlikowski, T.; Alexander, M. H. *J. Chem. Phys*. **1983**, *79*, 6006 and references therein.